

PAPER • OPEN ACCESS

## Design of a library using Matlab software for modeling and simulation of parabolic cylindrical solar collectors (CCP)

To cite this article: S A Sanchez *et al* 2020 *IOP Conf. Ser.: Mater. Sci. Eng.* **844** 012023

View the [article online](#) for updates and enhancements.

You may also like

- [NEAR-EQUIPARTITION JETS WITH LOG-PARABOLA ELECTRON ENERGY DISTRIBUTION AND THE BLAZAR SPECTRAL-INDEX DIAGRAMS](#)  
Charles D. Dermer, Dahai Yan, Li Zhang et al.
- [Design and Fabricated of improvement Parabolic Trough Solar Collector](#)  
M. A. Fayadh, A. F. Majeed and M. M. Walla
- [Classification of billiard motions in domains bounded by confocal parabolas](#)  
V. V. Fokicheva



The banner features the ECS logo on the left, a central portrait of M. Stanley Whittingham with a Nobel Prize medal, and a 'Register now!' button with a checkmark icon on the right. The background includes a photo of a conference audience and a hand holding a futuristic interface with various icons.

**ECS** The Electrochemical Society  
Advancing solid state & electrochemical science & technology

**242nd ECS Meeting**  
Oct 9 – 13, 2022 • Atlanta, GA, US  
Presenting more than 2,400 technical abstracts in 50 symposia

**ECS Plenary Lecture featuring M. Stanley Whittingham,**  
Binghamton University  
Nobel Laureate – 2019 Nobel Prize in Chemistry

**Register now!**

# Design of a library using Matlab software for modeling and simulation of parabolic cylindrical solar collectors (CCP)

S A Sanchez<sup>1</sup>, M A Quiroz<sup>1</sup>, LR Sierra<sup>1</sup>, A D Morales<sup>1</sup>, J M Palencia<sup>1</sup>

<sup>1</sup>Corporación Universitaria Antonio José de Sucre, Sincelejo, Colombia,  
Faculty of Engineering Science, GINTEING Research Group

sergio\_sanchez@corposucre.edu.co

**Abstract.** Much of the energy available to the earth comes from the sun, it is the largest source of radiation, emitting approximately 1353 W/m<sup>2</sup> of energy into the Earth's atmosphere, in the form of electromagnetic waves, with wavelengths ( $\lambda$ ) between 0,3 and 3  $\mu\text{m}$ . Within this spectrum we find the following radiations: Gamma (1%), Ultra violet (4%), Luminous (49%) and Infrared (46%). Only 51% of the solar radiation that enters the atmosphere reaches the earth's surface. This radiation represents a main source for renewable energy, presenting great applicability in solar thermal energy and specifically in the use of parabolic cylindrical solar collectors; that take advantage of this radiation to raise the temperature of a fluid, located in a receiving tube. The great problem of these systems is to generate a good design, which allows to reach high temperatures and good yields, therefore, many investigations have generated multiple design software, which mitigates the margin of error, but generally this software are limited; With licenses, they are complex and do not specify all the features for processing. The main objective of this research is an open source library that allows obtaining the highest efficiency of parabolic cylindrical collectors, based on the theoretical references Duffie, Beckman and Kalogirou. For this, the Matlab software and the Soltrace tool were taken into account, in order to validate the sizing and optical, thermal, geometric and global performance. Within the results, the maximum concentration ratio of the parabola is checked, which is obtained when the edge angle is 90 °. A functional library can be generated, where multiple measurements and shapes of the parabola were simulated, obtaining the highest overall performance, when the focal length is equal to the maximum height of the parabola, obtaining a performance of 62.64%.

## 1. Introduction

The sun is a sphere of gas from which a large amount of light and heat emanates. Life on Earth depends closely on the amount of solar radiation, is the largest star in the solar system, emits a plurality of electromagnetic waves, considering that energy as solar radiation, varies between ultraviolet rays far to gamma rays.

The sun is a black body whose surface temperature is 5,500 ° K, emits radiation continuously throughout the space, radiating approximately  $4 \times 10^{26}$  W. Due to this, the radiated solar energy is distributed as follows; Gamma (1%), Ultra violet (4%), Luminous (49%) and Infrared (46%), Gamma and ultraviolet radiation have a higher energy level, due to their low wavelength, and represents 5% of total solar energy.



The energy of the visible and infrared spectrum represents 95% of the total, and is the one that must be taken into account for its use. Of this large portion of energy that enters the atmosphere, only 51% reaches the surface of the earth, because 4% is reflected on the surface, 20% is reflected in the clouds, 6% is reflected in the atmosphere, and 19% is absorbed by the atmosphere and clouds. The radiations that reach the earth can be due to the albedo effect, direct or diffuse.

There are different types of energy sources; non-renewable and renewable; the non-renewable sources that are found in nature in a limited quantity and once consumed in their entirety, cannot be substituted, since there is no production or extraction system, for example; fossil fuels (coal, oil, natural gas) and nuclear fuels (uranium, plutonium, among others). On the other hand, there are renewable sources, which are those that are obtained from virtually inexhaustible natural sources, either because of the immense amount of energy they contain, or because they are capable of regenerating by natural means, for example; solar, wind, geothermal, hydroelectric, tidal, wave, biomass, among others.

The sun is one of the virtually inexhaustible renewable source, so it has multiple uses and applications, within the collection of solar energy can be divided into passive thermal collectors, active thermal collectors and photovoltaic collectors. For the particular case of this investigation, thermal energy will be studied in active thermal collectors, specifically in parabolic cylindrical solar collectors.

For a long time, solar collectors have been objects of study within the use of solar thermal energy, in the 19th century the first investigations were initiated to apply and develop technologies that would allow this energy to be used as a caloric and electrical source on a commercial scale and massive, [1] qualifying it as a new alternative of renewable energy, solar thermal energy defines the release of heat in a system, this heat is transferred from a hotter body to another that has less heat, so that, while more heat be introduced, the higher the temperature until a phase modification is reached, this is widely used to change from liquid to gaseous state and for any state of matter [2].

Such investigations caused the invention of various systems for the use of solar energy from the sun, obtained by means of solar panels and mirrors, so that the mirrors, concentrate the light in a receiver that reaches temperatures of 1,000 ° C, heat produced is used to heat a fluid that generates steam, important for multiple uses and derivative systems [3], however, for the collection and concentration, not only enough with common mirrors, so the design of these solar collectors has changed, highlighting the most used today; cylindrical parabolic collectors, central tower collectors, stirling, composite, semi-parabolic collectors, among others.

The parabolic cylindrical collectors are linear-focus solar collectors, which transform direct solar radiation into thermal energy, thanks to the heating of a working fluid that can reach 400 ° C in very favorable cases, within their applications they are found, drinkable water, disinfection, evaporation drying and distillation, among others.

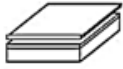


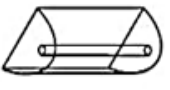

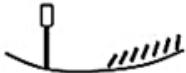
Taking into account that, in 1866, Auguste Mouchout used parabolic trough collectors (CCP) to move a steam engine, that same year the first patent of a solar collector was granted and in subsequent years John Ericsson or Frank Shuman designed systems and plants complete for irrigation, refrigeration, and locomotion. Between 1984 and 1991, in the Mojave Desert (California), 9 plants known as SEGS (Solar Energy Generating Systems) with an installed capacity of 354 MW were built and connected, with these plants being the only commercial centers built until 2007 [4] in Spain, in 2008 the construction of Andasol 1 began, one of three 50MW power plants very similar to each other, being considered as the true beginning of the rebirth of the generation of solar thermal energy worldwide, since 2013 the SENER trough is the collector that is most frequently built today; However, for the modeling of these solar collection systems it includes the study of different designs, the geometric, optical and thermal parameters being relevant, which have a detailed and specific study related to theoretical-analytical thermodynamics, optical principles and geometric analysis [5].

Currently, there are different software that facilitate the design of libraries for solar collectors, including SPSS, Staca, SAS, R, model, soltrace among others. The relevance of this research is to achieve an open source library, scalable, functional, versatile, simple to use and mainly to obtain efficient prototypes.

**2. Fundamentals**

Solar collectors are elements that capture solar radiation and convert it into thermal energy, that is, they generate heat [6], they are composed of a flat or curved plate, of reflective material that direct and concentrate the light beams, in addition, of a receiver that receives concentrated energy by adsorbing the greatest amount of energy to convert it into heat, generating high temperatures [7].

To reach high temperatures in the collectors, it is important to modify the collection system, so that the concentration is increased, which leads to different types of collectors for each application, in the following section, we will observe the types of solar collectors in function of temperature ranges and solar concentration ratio.

		Name	Sketch	Concentration reason "C"	Temperature range reached [C°]	
Stationary	Flat adsorber	Flat water collector		$C \leq 1$	$30 < T < 250$	
		Empty tubes		$C \leq 1$	$50 < T < 200$	
Followers	Track an axis	Compound parabolic collector CPC		$1 < C < 15$	$70 < T < 300$	
		Parabolic cylindrical collector PCC		$15 < C < 40$	$70 < T < 350$	
	Two axis tracking	Point adsorbents	Parabolic disc		$100 < C < 1000$	$70 < T < 1500$
			Central tower		$100 < C < 1500$	$150 < T < 1500$

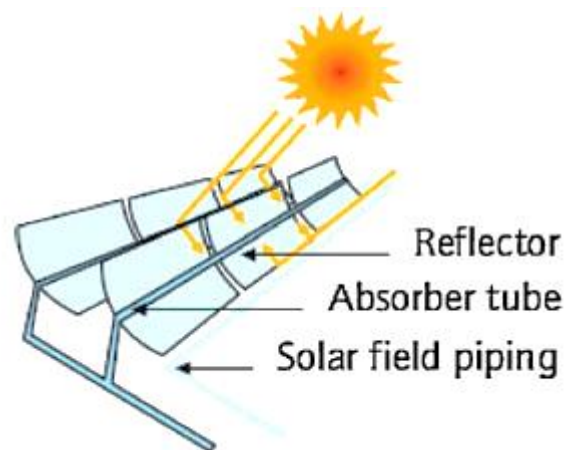
**Figure 1.** Classification of collectors according to the concentration factor.

As can be seen in the image, the classification of solar collectors, where static collectors and followers, their respective subclassifications and the concentration ratio are more clearly denoted. On the other hand, the figure defines the attainable temperature range, where it is evident that the central tower collectors are the ones that can achieve higher temperatures, but their installation and sizing are more expensive compared to the others.

The performance of the systems is given by the typology of the concentrator, but also by the fluid used. However, it can be determined that the yield increases with concentration [8].

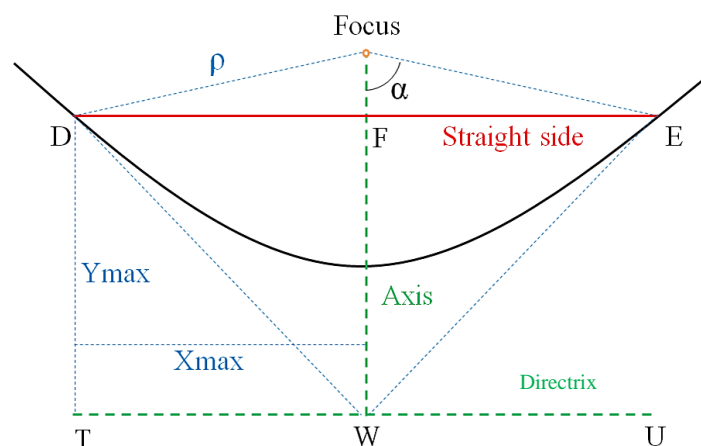
### 2.1. Parameters of cylindrical parabolic collectors or CCP.

Parabolic cylindrical collectors have shown in real systems efficiencies of between 10 and 15%, reaching maximum yields of up to 21.5% in any of the SEGS plants, currently the fluids used in the receiving tube are synthetic oils that can exceed 400 ° C. The CCP are composed of different parts, one of them is the geometric shape of a parabola, so that all the rays affect the focus of it, taking advantage of a much larger area where the sun's rays would be reflected, with the capacity of absorbing heat, where thermal energy is obtained that will be transformed later.



**Figure 2.** Parts of the parabolic cylindrical parabolic.

In Figure 3, the different parts of a parabolic cylindrical solar collector are appreciated; the parabolic reflector, the receiver tube and the pipes; All these elements play an important role in increasing thermal energy. When observing the collector transversely, we observe a parabola that is characterized by certain parameters, defined below.



**Figure 3.** Geometric parameters of a parabola.

In Figure 3, the main parameters of a solar collector are specified, which defines  $\rho$  as the distance from the focus to the edge of the collector,  $\alpha$  as the angle of incidence, the straight side that corresponds to the width of the collector,  $Y_{max}$  to the maximum height of the collector and  $X_{max}$  the maximum width of half a parabola.

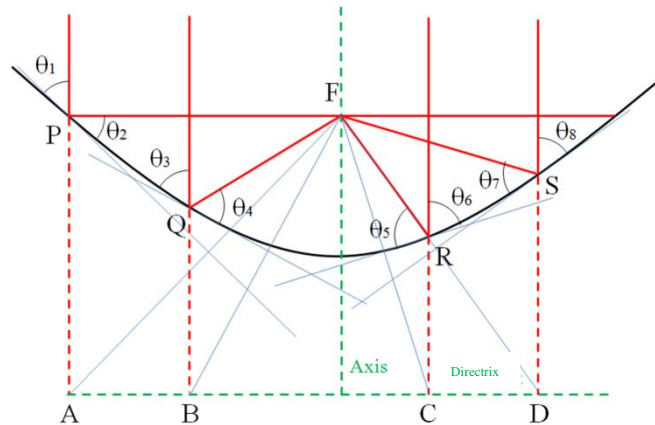
The conditions of the CCP models implemented for the design of the proposed library favor collectors with an incidence angle of 90 ° ( $\alpha$ ), to reach the highest solar concentration, according to the theoretical reference Kalogirou, the geometry of the CCP it is calculated based on the focal length, so that the straight side (Fig. 5) is 4 times the focal length.

$$L_{recto} = 4 * D_{foco} \tag{1}$$

The parabola defines an  $X_{max}$ , described as the maximum distance of half a parabola, therefore.

$$x_{max} = \frac{L_{recto}}{2} \tag{2}$$

To corroborate the parameters of the parabola, the manual geometric method was analyzed, by method of guidelines and the crossing point of perpendicular points on the directrix, through the focal length and any point of a directrix [9].



**Figure 4.** Principle of bisector and reflection.

In the red lines A, B, C and D, the principle of reflection on a flat surface is observed, where, the same angle of incidence  $\theta_1$  is equal to the angle of reflection  $\theta_2$ , so the reflections are directed to the focus, at any point of the curved line. Likewise, with the bisectors (blue lines) are the points P, Q, R, S, which draw the curved line, which as it is constructed, the parameters of Figure 4 are observed.

For the construction of the parabola by means of the library, equation 3 was used, taking samples from  $-X_{max}$ , to  $X_{max}$ , finding Y in the Cartesian plane, such samples end until reaching  $Y_{max}$  in this case.

$$Y = \frac{x^2}{4 * D_{foco}} \tag{3}$$

It is also necessary to find the distance of the curved side of the parabola from its vertex to its  $X_{max}$ , so that:

$$S = \int_0^{X_{max}} \sqrt{1 + \frac{X_{max}^2}{4 * D_{foco}^2}} \tag{4}$$

The incident angle is not always 90 °, nor is the distance  $\rho$  equal to  $X_{max}$ , these parameters are defined in equation 5 and 6.

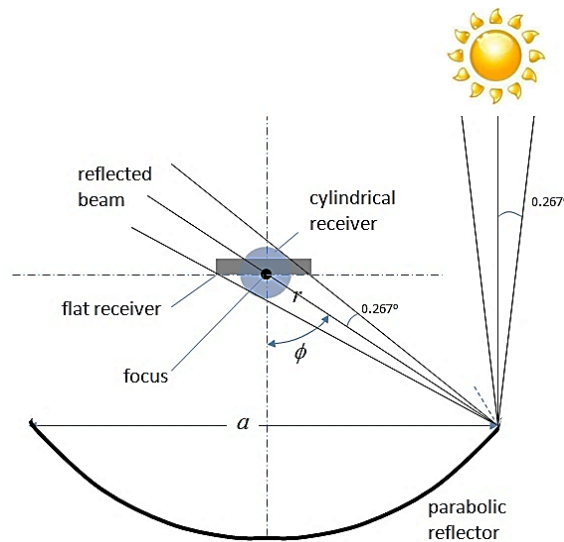
$$\alpha = \tan^{-1}\left(\frac{X_{max}}{D_{foco} - Y_{max}}\right) \tag{5}$$

$$p = \sqrt{X_{max} + (Dfoco - Y_{max})^2} \tag{6}$$

With the defined equations of the reflective area, we will design the receiver tube.

**2.2. Receiver tube**

For the design of the receiver or adsorbent tube it is necessary to take into account that the sun does not emit its energy in a timely manner, observed from the earth's surface, it is known that the solar disk corresponds to the projected area for an opening angle of 32 ° and does not emit its rays in parallel, however, they are distributed over a cone of solid angle directions of 16 °, which means that the rays do not reach the diameter of the larger receiver. [10], this is known as the cosine effect, as evidenced in Figure 5.



**Figure 5.** Solar projection.

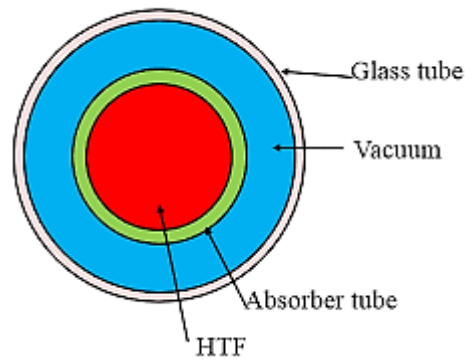
The linear CCP receiver is the element that converts concentrated solar radiation into thermal energy, through a fluid. This is located on the focal length of the parabolic trough concentrator, being decisive for the overall performance of the collector [11]. Within the receiving tube, the working fluid is important, depending on the temperature that is intended to be reached and can be reached, as indicated in Table 1 below.

**Table 1.** Fluid temperatures in the manifold.

Fluid	Temperatures
<b>Demineralized water</b>	T < 200 °C
<b>Synthetic oils</b>	200 °C < T < 450 °C
<b>Santotherm 55</b>	T. Máx a 300 °C
<b>Monsanto VP-1</b>	T. Máxa 400 °C
<b>Syltherm 800</b>	T. Máxa 425 °C

There are different types of receiver tube design, the most efficient are those that work under the greenhouse effect principle, because of the temperature they can reach. This research focuses on this type of tubes.

This type of receiver tube consists of two tubes: one metallic interior (through which the fluid that heats up circulates) and another glass exterior (Figure. 6).



**Figure 6.** Parameters of a receiver tube.

To calculate both diameters it is necessary to apply the following equations with respect to Figure 6.

$$D_{min} = X_{max} * \frac{\sin(0.267)}{\sin\left(\frac{\alpha}{2}\right)} \quad (7)$$

$$D_{max} = X_{max} * \frac{\sin\left(0.267 + \frac{1.15}{2}\right)}{\sin\left(\frac{\alpha}{2}\right)} \quad (8)$$

To calculate the thermal concentration factor for the adsorbent tube it is necessary to know the areas of both cylinders, like this:

$$FC = \frac{A_{capt}}{A_{total}} \quad (9)$$

Being, ( $A_{capt}$ ) the catchment area and ( $A_{total}$ ) the area of the receiving tube.

In addition, it is also necessary to calculate the amount of accumulated soles ( $C_{max}$ ) and the volume ( $Vol$ ) of the receiver area, defined as follows:

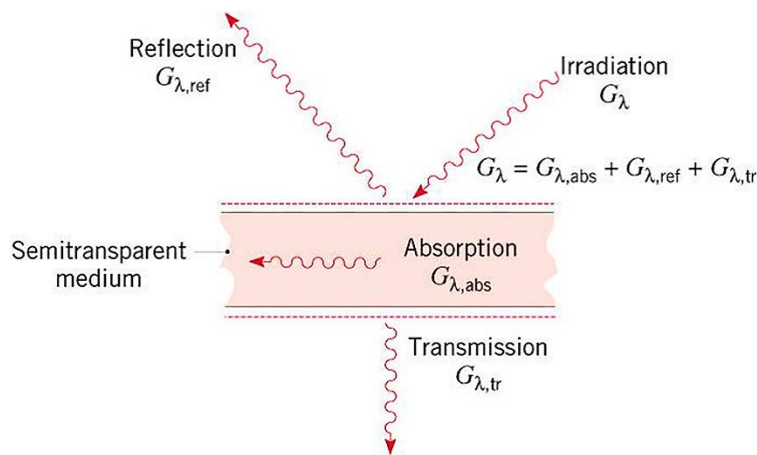
$$C_{max} = X_{max} * \frac{2 * L}{D_{tubo} * L} \quad (10)$$

$$Vol = 1000 * \pi * \left(\frac{D_{max}}{2}\right)^2 * L \quad (11)$$

Being ( $L$ ) the length of the collecting tube and ( $D_{tubo}$ ), the diameter of the receiving tube of the market.

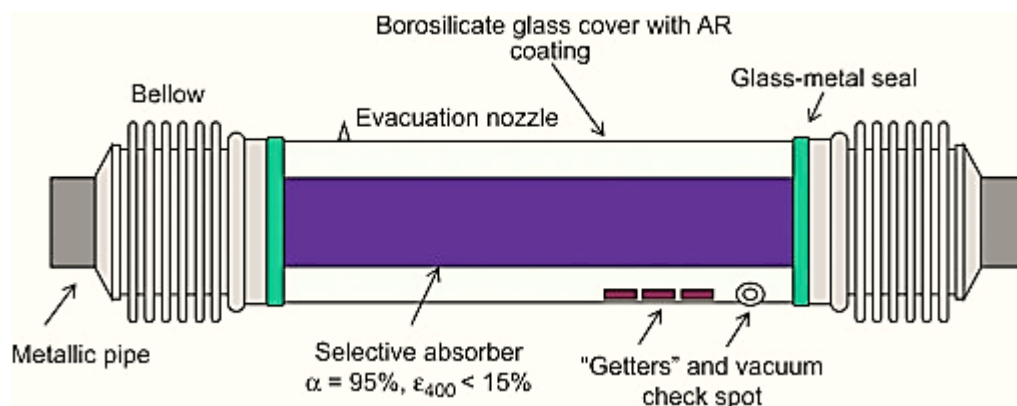
On the other hand, it is important to take into account in the receiver tube the transfer of heat by radiation, where some surface properties such as; emissivity, absorptivity and reflectivity. There is another property, transmissivity, which is usually of little importance. This can be corroborated in Figure 7.





**Figure 7.** Radiation heat transfer.

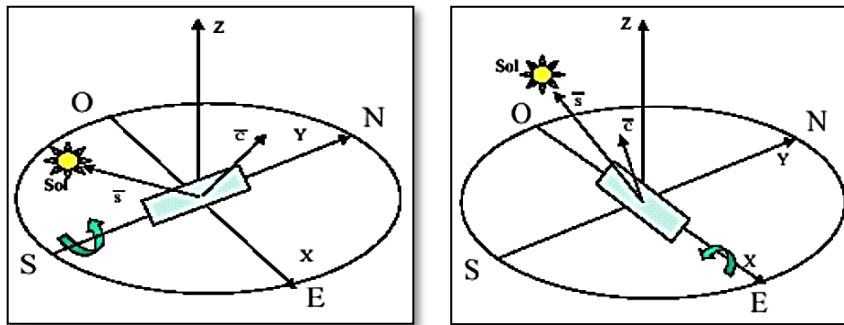
The metal inner tube has a selective coating that has a high absorptivity ( $\sim 94\%$ ) and a low emissivity in the infrared spectrum ( $\sim 15\%$ ). Most of the coatings degrade in contact with the air, when they are hot, so it is required that there is a high vacuum in the chamber that is between the inner metal tube and the glass cover, in addition it usually takes an anti-reflective treatment on both sides, to increase its transmissivity, consequently, the optical performance of the collector. In Figure 8, the parts of a receiver tube are observed.



**Figure 8.** Parts of a receiver tube.

### 2.3. CCP requirement.

Normally, CCPs are installed in such a way that their axis of rotation is oriented in the East-West or North-South direction, although intermediate orientations could also be used, and thus obtain the greatest possible solar utilization and increase their overall performance [12] [13]. As seen in figure 9.



**Figure 9.** North-South and East-West Orientation.

In the process of thermal use of direct solar radiation by the CCP, a series of losses appear. These losses can be divided into three groups: optical losses, thermal losses and geometric losses. On the other hand, with losses, yields can be determined.

**2.4. Losses of solar collectors**

When solar radiation reaches the earth's surface, a large amount of this energy is lost due to different aspects, these losses can be divided into 3 groups; optical, geometric and thermal losses.

Optical losses occur when not all the energy that reaches the area of the reflector (parabola) reaches the fluid that circulates inside the receiver tube, these losses originate for different reasons; initially because the area of the reflector is not a perfect mirror, producing losses due to reflectivity ( $\rho$ ), transmissivity ( $\tau$ ), absorptivity ( $\alpha$ ) and losses that occur due to intrinsic imperfections of the material, called the interception factor ( $\gamma$ ).

The geometric losses occur due to the angle of solar incidence on the collector, within these losses is the cosine effect, lost by the end of the collector, lost by shadows and lost by the purely optical properties of the collector.

Thermal losses are caused by the difference in ambient temperatures and the average temperature of the fluid that travels through the receiver tube, within these losses is found by radiation, by convection and conduction of the materials that make up the collector.

**2.5. Performance of solar collectors**

Not all incident solar power will be transformed into useful thermal power in the fluid that travels through the receiving tube. Due to the different losses experienced by solar collectors. There are 4 types of returns; optical ( $\eta_{opt}$ ), geometric ( $\eta_{geo}$ ), thermal ( $\eta_{term}$ ) and global ( $\eta_{global}$ ). In the following equations the different yields are described.

$$\eta_{opt} = \rho * \gamma * \tau * \alpha * F_{limp} \tag{12}$$

In equation 12 the optical performance ( $\eta_{opt}$ ), is described as the product of the reflectivity ( $\rho$ ) of the reflector area, transmissivity ( $\tau$ ) of the glass cover, the absorptivity ( $\alpha$ ) of the receiving tube and fouling factor ( $F_{limp}$ ) of the installation.

$$\eta_{geo} = K(\theta) * F_{sombras} \tag{13}$$

In equation 13, the geometric performance ( $\eta_{geo}$ ), is described as the product of the angle of incidence modifier ( $K(\theta)$ ) and the shadow factor ( $F_{sombras}$ ).

$$\eta_{term} = \frac{Q_{util}}{DNI * A_{aper} * \eta_{opt} * \eta_{geo}} \quad (14)$$

In equation 14, the thermal efficiency ( $\eta_{term}$ ) is described as the ratio between useful heat ( $Q_{util}$ ) received by the fluid that travels through the receiving tube and the product of the solar irradiation of the place where the collector is located (DNI), the reflector aperture area ( $A_{aper}$ ), optical performance ( $\eta_{opt}$ ) and geometric performance ( $\eta_{geo}$ ).

$$\eta_{global} = \frac{Q_{util}}{DNI * A_{aper}} \quad (15)$$

### 3. Methodology

The proposed library for the design of parabolic cylindrical solar collectors, is characterized according to the factors that affect the sizing, conditions and limitations of these, based on theoretical references that propose designs of solar collectors, in addition to the mathematical relationships that affect in the calculation of its performance, applying the optical, geometric and thermal principles that interact, which make up the overall efficiency of the collector based on the estimated solar radiation during the day.

The Matlab Software version 8.5 R2015b with professional license and as a complementary tool Soltrace was used for the design of the library, which is a software developed at the National Renewable Energy Laboratory (NREL) to model solar concentration systems (CSP) and analyze its optical performance. It is ideal for solar applications, the code can also be used to model and characterize many general optical systems.

**Table 2.** Shows a comparative chart of different software that is used for the design of parabolic cylindrical solar collector libraries.

Software	Learning curve	Data management	Gráficos
SPSS	Gradual	Moderate	Good
Stafa	Moderate	powerful	Good
SAS	Steep	Very powerful	Very good
Modelica	Steep	Very powerful	Very good
R	Steep	Very powerful	Excellent
Matlab	Steep	Very powerful	Excellent

Different software was validated, according to its versatility and functionality, so Matlab was chosen due to its scientific approach, the use of matrix expressions and vector arrangements, the different tools (toolbox) that facilitate complex analyzes, its ease to integrate flows of works with other hardware, with other environments, its analysis in the cloud and finally, for being reliable and fast.

The library has all the equations listed in the previous sections, it should be noted that the measures are handled in the International System of Units.

When executing the library, the focal length, the length of the reflective area and the adsorbent tube must be specified with their respective diameter based on the technical characteristics. Then, there is the straight side and therefore, Xmax, Ymax and the curved side, based on equations 1-4.

Subsequently, there is the area of the reflecting surface and the collection area, the opening angle ( $\alpha$ ) and distance  $\rho$  (Figure 4) of the CCP, corresponding to equations 5 and 6.

The minimum and actual diameter of the absorbent tube is calculated, based on equations 4 and 5, of Figure 6.

It is very important to know other parameters, such as the thermal concentration factor and the amount of accumulated soles, defined by equations 7, 8 and 9, based on figures 1, 5, 6, and 7. On the other hand, it is necessary validate the solar irradiation in the place where the solar collector is going to be located, and check the solar behavior during the 12 months of the year. In order to identify which are the most favorable and least favorable months.

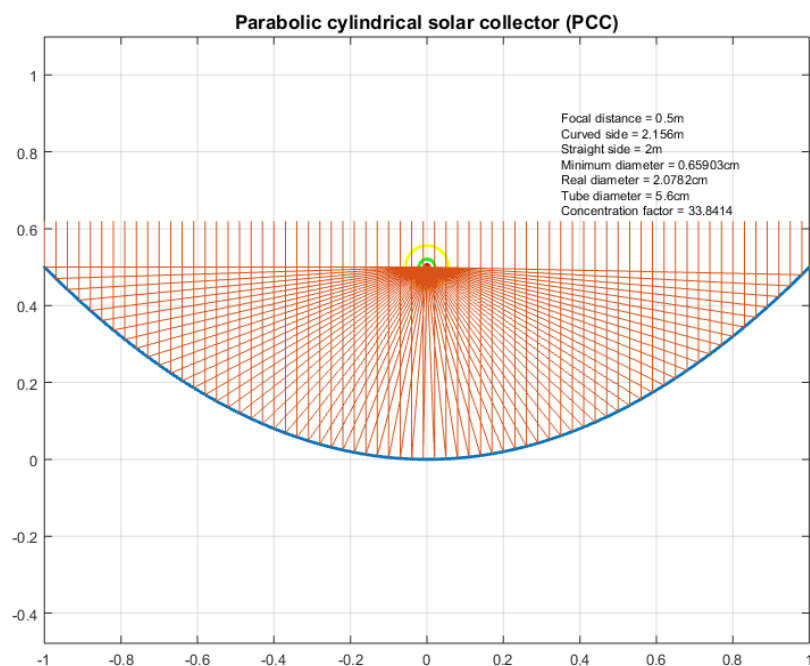
The design of the collector was conditioned to the dimensions of the standard vacuum receiver tube, which has a structural specification of 1.8 m long and a diameter of 5.6 cm.

For the validation of the library, different tests were performed using the initial parameters described in Table 3, with the purpose of reviewing the mathematical equations mentioned above, based on the theoretical references Duffie, Beckman and Kalogirou.

**Table 3.** Parameters obtained by the library in Matlab.

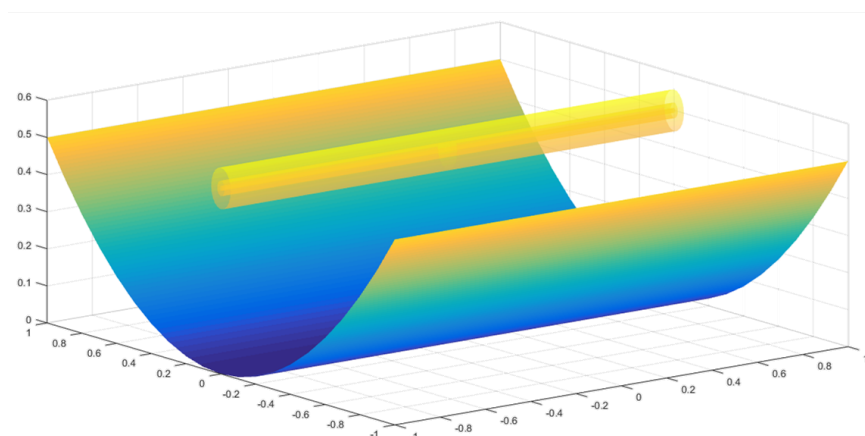
Variable	Valor	Unidad	Descripción
<b>Dfoco</b>	0.5	m	Focal distance
<b>Largo</b>	1.8	m	Receiver tube length
<b>Dtubo</b>	0.056	m	Tube diameter of the market.
<b>Largo2</b>	2	m	Collector Length
<b>Lrecto</b>	2	m	Distances straight side of the parabola
<b>Xmax</b>	1	m	Distance from the vertex to the side of the collector
<b>Ymax</b>	0.5	m	Manifold height
<b>Lcurvo</b>	2.1560	m	Curved side distance of the parabola
<b>Asurf</b>	4.3112	m	Reflective surface area
<b>Acapt</b>	4	m	Collection area or collector opening.
<b>P</b>	1	m	Distance from the edge of the parabola to the focus.
<b>A</b>	90	Grados	opening angle
<b>Dprop</b>	0.0066	m	Minimum tube diameter
<b>Dprop2</b>	0.0207	m	Real tube diameter
<b>Dpropcm</b>	0.65	cm	Minimum tube diameter
<b>Dprop2cm</b>	2.07	cm	Real tube diameter
<b>Atotal</b>	0.1182	m <sup>2</sup>	Actual collector tube area
<b>Fm</b>	0.5104	m	Average distance between surface and receiver
<b>Io</b>	-1.0184	m	Lost distance in the absorber tube
<b>Ae</b>	-2.0368	m <sup>2</sup>	Lost area absorbing tube
<b>FC</b>	33.84	Adi.	Concentration factor
<b>Cmax</b>	35.7143	Adi	Amount of accumulated soles
<b>Vol</b>	0.6106	litros	Tube and liquid volume
<b>Emisv</b>	0.09	decimal	Emissivity of the reflective surface
<b>Absrt</b>	0.96	decimal	Absorptivity
<b>Rflec</b>	0.935	decimal	Reflectivity of the reflective surface
<b>Transm</b>	0.96	decimal	Transmissivity of the absolute tube

Based on the result obtained by table 1, after varying the focal length between (0.4 - 0.6 m), maintaining the initial parameters, the author Kalogirou's theory is fulfilled; when the focal length is equal to the height of the collector, a higher overall efficiency is obtained. As shown in Figure 18. Regarding geometric, thermal and optical losses, it was taken into account that the receiver tube had a smaller distance based on the length of the collector, to avoid losses due to the end of the collector, in addition to the characteristics of Emissivity, absorptivity and reflectivity of the reflective area material are theoretically good. The following figure shows the behavior of the light beams reflected in the area of the reflector, over the focal length.



**Figure 10.** 2D image solar collector with 0.5m focus.

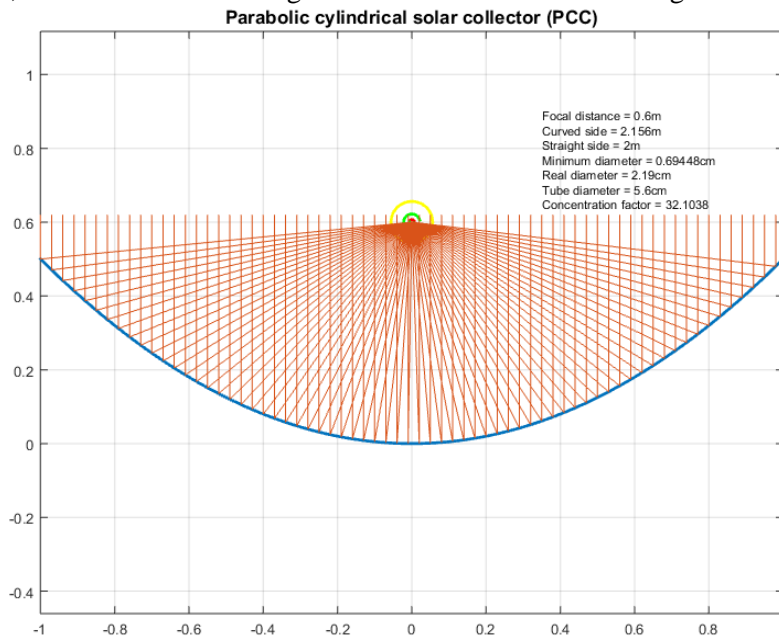
Based on the results obtained in Figure 10, it is observed that all the light beams that are reflected in the area of the reflector, all are redirected to the focus of the parabola, this principle is fulfilled because the focal length  $e$  is equal at the height of the collector, that is, the angle of solar incidence is  $90^\circ$ .



**Figure 11.** 3D image solar collector with 0.5m focus.

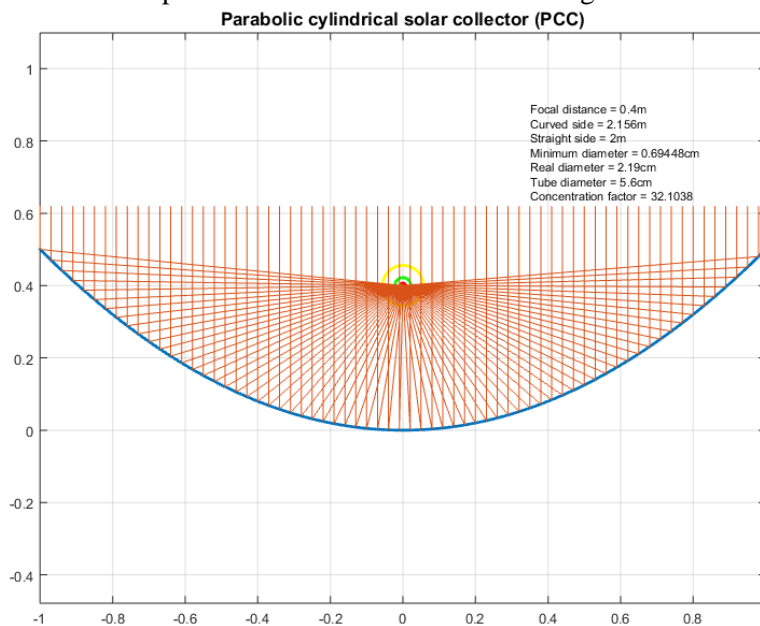
In figure 11, it is observed that theoretically all the light beams are concentrated in the receiving tube, because it is located exactly in the focus of the parabola, where it is evidenced that there is a higher concentration of heat, observing a yellow color, and in the parts where the blue color is observed, it is due to shadows caused by the receiving tube.

In Figure 12, we observe a focal length of 0.6 m and a maximum height of 0.5 m.



**Figure 12.** 2D image solar collector with focus higher than agreed.

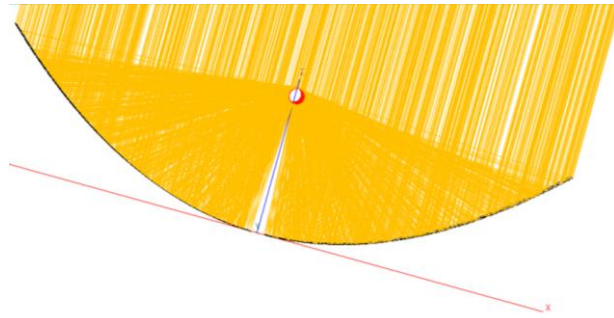
With respect to Figure 12, it can be seen that most of the light beams are not satisfactorily reflected towards the focus, which affects the concentration factor. In Figure 13, the focal length is 0.4 m compared to the maximum collector height that is 0.5m.



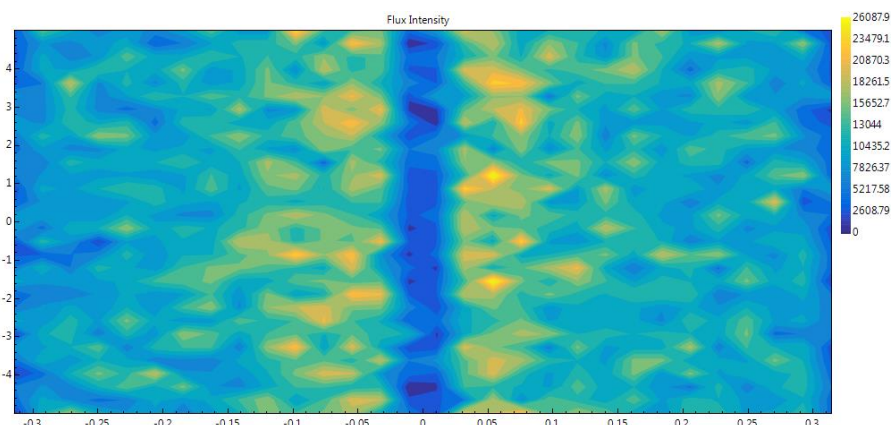
**Figure 13.** 2D image solar collector with lower focus than agreed.

Similarly, in Figure 13, the same phenomenon in Figure 12 occurs, all the light beams do not reach the focus, that is to say the receiving tube, which directly affects the concentration factor.

With the SolTrace software, the solar behavior of the incident beams and the flow map is illustrated in more detail, where it is observed that, with a solar acceptance angle of 90 degrees, it is theoretically guaranteed that all the light beams that project in focus. As illustrated in Figure 14 and 15.



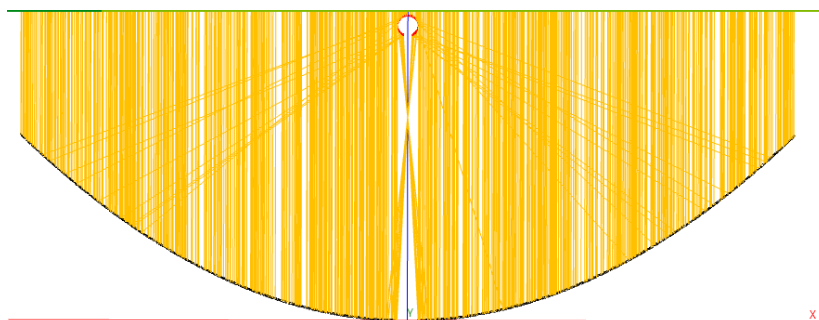
**Figure 14.** Solar Analysis in SolTrace software with a focal length of 0.5 m.



**Figure 15.** Flow map in the SolTrace software with a focal distance of 0.5m.

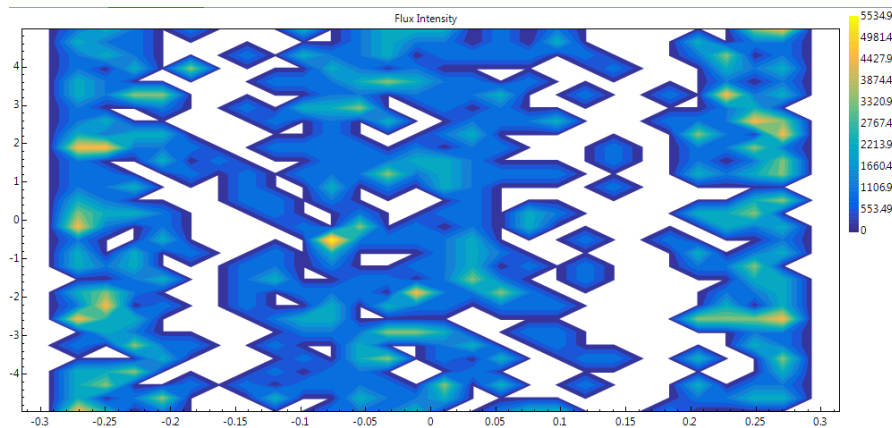
All the incident light beams are satisfactorily reflected, obtaining the highest solar collection by the receiving tube, therefore, the maximum performance. In the figure of the flow map, it is evident that the points with blue color are caused by shadows and in the more yellow ones, where solar radiation is more reflected.

In Figure 16, a focal length is shown, higher compared to the height of the collector.



**Figure 16.** Solar Analysis in SolTrace with focus greater than defined.

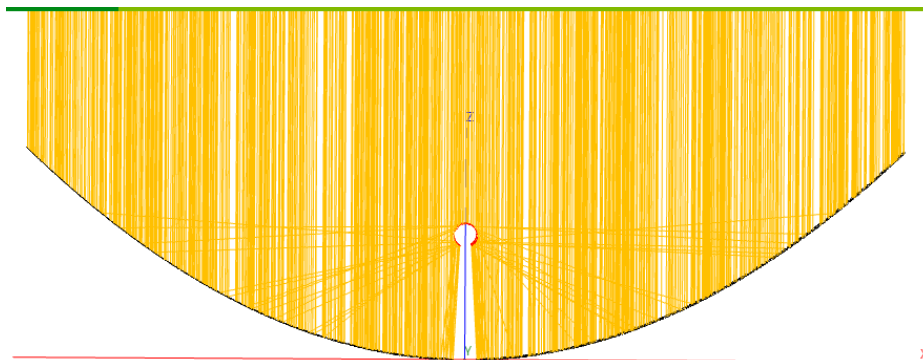
It is observed in Figure 16, that many of the solar rays that affect the area of the reflector do not reach the focus, due to the cosine effect and the location of the focus. Which allows the overall collector performance to decrease. Figure 18 shows the flow map of Figure 17.



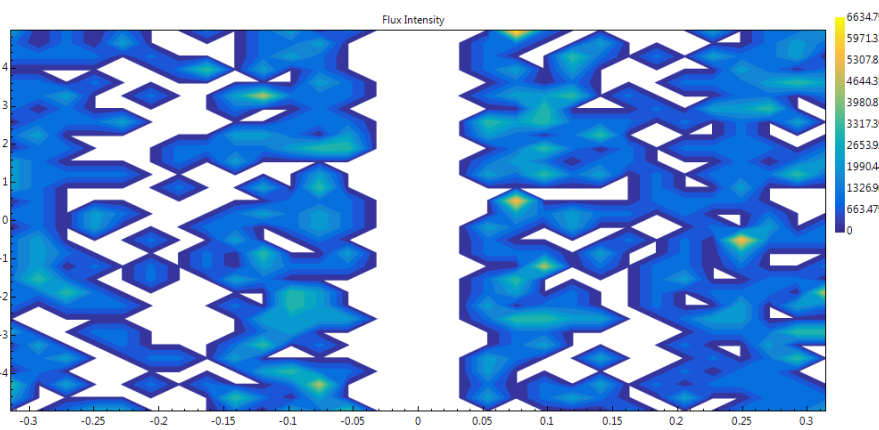
**Figure 17.** Flow map in SolTrace with focus greater than defined.

When observing the previous image, it shows the lack of solar concentration in the receiving tube, in addition there is little solar concentration.

In figure 18 and 19 a focal distance is observed that is located inside the solar collector, presenting a phenomenon similar to figures 15 and 16, where the rays reflected in the area of the reflector, do not reach to focus on the focus.



**Figure 18.** Solar Analysis in SolTrace with focus less than defined.



**Figure 19.** Flow map in SolTrace with focus less than defined.



It shows more spaces with shadows and low heat concentration, which causes the overall efficiency of the collector to decrease considerably.

Table 4 shows the optical, thermal, geometric and global yields of a solar collector test with the library, varying the focal length.

**Table 4.** Performance of the solar test collector, with different focal distances.

	<b>0.4 m focal length</b>	<b>0.5 m focal length</b>	<b>0.6 m focal length</b>
<b>Variable</b>	value	value	value
<b>Nopt</b>	0.8617	0.8617	0.8617
<b>Ngeo</b>	0.5823	0.7270	0.6354
<b>Nterm</b>	0.9556	1	0.9732
<b>Nglobal</b>	<b>0.5099</b>	<b>0.6264</b>	<b>0.5564</b>

In table 4, it can be corroborated that a solar collector with an acceptance angle of 90 degrees, allows to increase the overall efficiency of the collector, it is important to take into account that these systems are exposed to different losses, so it is essential to define a Good structural design, relevant materials and good software that facilitates calculations and reduces physical tests that increase costs.

#### 4. Conclusions

The library developed in Matlab software and verified with the complementary tool Soltrace, allowed to simplify the process of design of parabolic trough collectors, creating a functional model that allows simulating the relevant variables to find the performance based on solar radiation.

The development of this methodology allowed to analyze in detail the variability of some factors, allowing to select the appropriate components and obtain yields adjustable to the local environmental conditions of the implementation. In addition, the expected behaviors for each of the variables were obtained, taking into account the theoretical references, where it was validated that the focal length should have the same measure as the maximum height of the collector, so that the angle of solar incidence is 90 degrees. This allows the overall collector performance to be the most efficient.

The dimensions must be adjusted to the measurements of the receiver tube and the most optimal focal length, to achieve maximum solar concentration in the absorber tube fluid. As future work, this library is expected to be validated with a practical prototype, in order to better optimize losses and yields in different contexts.

#### [References

- [1] Ideam.gov.co. (2019). RADIACIÓN SOLAR - IDEAM. [online] Available at: <http://www.ideam.gov.co/web/tiempo-y-clima/radiacion-solar> [Accessed 14 Jul. 2019].
- [2] Como-funciona.co. (2019). ENERGIA TÉRMICA | Características, ejemplos y funcionamiento. [online] Available at: <https://como-funciona.co/la-energia-termica/> [Accessed 14 Jul. 2019].
- [3] Acciona.com. (2018). ¿Qué beneficios tiene la energía solar? | ACCIONA. [online] Available at: <https://www.acciona.com/es/energias-renovables/energia-solar/> [Accessed 10 Jul. 2019].

- [4] Villasante, C. (2010). [online] Sc.ehu.es. Available at: [http://www.sc.ehu.es/sbweb/energias-renovables/temas/termoelectrica/revision/Articulo\\_Revision\\_Tecnologias\\_Solares\\_Termoelectricas\\_.pdf](http://www.sc.ehu.es/sbweb/energias-renovables/temas/termoelectrica/revision/Articulo_Revision_Tecnologias_Solares_Termoelectricas_.pdf) [Accessed 8 Jul. 2019].
- [5] Taylor & Francis. (2007). Object oriented modelling and simulation of parabolic trough collectors with modelica. [online] Available at: <https://www.tandfonline.com/doi/abs/10.1080/13873950701847199> [Accessed 8 Jul. 2019].
- [6] Solar-energia.net. (2019). Colector solar. [online] Available at: <https://solar-energia.net/definiciones/colector-solar.html> [Accessed 9 Jul. 2019].
- [7] VELASCO, C. (2012). DISEÑO DE CAPTADOR SOLAR CILÍNDRICO PARABÓLICO. [online] Available at: [http://oa.upm.es/14011/1/PFC\\_CARMEN\\_PAREDES\\_VELASCO.pdf](http://oa.upm.es/14011/1/PFC_CARMEN_PAREDES_VELASCO.pdf) [Accessed 6 Jul. 2019].
- [8] Laenergiasolar.org. (2018). Colector Cilindro Parabólico: ¿qué es y cómo funciona? - La Energía Solar. [online] Available at: <https://www.laenergiasolar.org/energia-termica-solar/colector-cilindro-parabolico/> [Accessed 15 Jul. 2019].
- [9] Sastre Alfaro, A. (2016). ANÁLISIS DE COLECTORES SOLARES DE MEDIA TEMPERATURA. Leganés. [Accessed 15 Jul. 2019].
- [10] Cherian, R. (2016). Performance Enhancement of Solar Water Heater using Compound Parabolic Reflector and Numerical Simulation of Thermal Losses. [Accessed 7 Jul. 2019].
- [11] Busso, MSc. Arturo (2019). Estudio y caracterización de un colector plano. [online] Available at: [http://exa.unne.edu.ar/investigacion/energia\\_solar/PUBLICACIONES/informe\\_PI455.pdf](http://exa.unne.edu.ar/investigacion/energia_solar/PUBLICACIONES/informe_PI455.pdf)
- [12] J. Roviras, V. Sarrablo, M. M. Casanovas (2016). Integración arquitectónica de colectores solares térmicos cerámicos para clima mediterráneo.
- [13] Rodríguez, Juan. (2015). Energía solar, Medio Ambiente y desarrollo. [online] Available at: [http://www.guzlop-editoras.com/web\\_des/ener01/enersolar/pld0524.pdf](http://www.guzlop-editoras.com/web_des/ener01/enersolar/pld0524.pdf). [Accessed 15 Jul. 2019].